

СООБЩЕНИЯ
ОБЪЕДИНЕННОГО
ИНСТИТУТА
ЯДЕРНЫХ
ИССЛЕДОВАНИЙ

Дубна

95-147

E13-95-147

L.M.Soroko

ISOPLANATIC MESO-OPTICAL
FOURIER TRANSFORM MICROSCOPE
FOR NUCLEAR EMULSION

1995

I. INTRODUCTION

It was shown in [1,2] that the problem of the coma aberrations in optics, holography and meso-optics can be solved by using the generalized Abbe sine condition and the Welford theorem about the form of the hologram's backing. In this line the isoplanatic meso-optical Fourier transform microscope (MFTM) for nuclear emulsion has been proposed.

Recall that any meso-optical mirror with ring response, installed in the MFTM, produces two meso-optical images of the particle track having small dip angle. The main technological disadvantage of such a device is very large geometro-optical aberrations, observed in the meridional cross section of the microscope [3]. Due to this feature the diameter of the meso-optical mirror with ring response must be as large as 160 mm. To reduce the overall dimensions of the MFTM, the initial meso-optical mirror from metal must be replaced by the equivalent aplanatic meso-optical hologram with ring response. The form of the hologram's backing is defined by Welford's theorem [4], and can be chosen a spherical one with curvature radius R defined by the equation [4] (Fig. 1)

$$\frac{1}{R} = \frac{1}{l_1} + \frac{1}{l_2}, \quad (1)$$

where l_1 and l_2 are distances from the reference object point to the hologram and from the hologram to the meso-optical image, respectively. The sines of l_1 and l_2 are chosen in accordance with general rules in optics. For $l_2 \gg l_1$, $R \approx l_1$. Thus in this extreme case the aplanatic meso-optical hologram with ring response can be made on a spherical backing with center of the sphere being practically in the reference position of the particle track in the median plane of the nuclear emulsion layer (Fig. 2). The coma aberrations can be reduced in the ratio 5:1 and the overall dimensions of the aplanatic meso-optical element with ring response can be made reduced from the initial diameter 160 mm to about 35 mm.

In this paper we give the description of some new approaches to solve the problem of the coma aberrations in the meso-optical Fourier transform microscope (MFTM) for nuclear emulsion. The comprehensive analysis of the technological aspects of the experimental realization of some microscopes is presented. The theory of the multi-element isoplanatic mirror of the MFTM is developed.

II. TECHNOLOGICAL ASPECTS

A device designed for production of the meso-optical hologram with ring response on the spherical backing is shown in Fig. 3. The light source 1 produces two mutually coherent light beams, one convergent and another divergent. The real focus of the convergent beam is in the reference position of the particle track 0 in the median plane of the nuclear emulsion layer. The spherical shutter 2 has an open aperture in the form of a narrow sector with center on the optical axis of the frontal lens 4. The

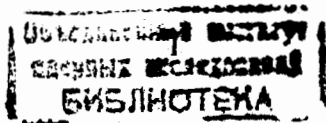


Fig. 1. Aplanatic meso-optical hologram with a ring response in the MFTM: 1 - source of the convergent light beam, 2 - aplanatic meso-optical hologram with a ring response on the nonplane backing, 3 - matrix photodetector of the meso-optical images, Я.Ф. - nuclear emulsion layer, R - curvature radius of the hologram backing, having axial symmetry with respect to the optical axis of the MFTM, $R^{-1} = l_1^{-1} + l_2^{-2}$, where l_1 and l_2 are the distance from the particle track to the hologram and from hologram to the matrix photodetector, O is the point in the meridional cross section on the marginal optical axis of the MFTM, on which the center of the circle of radius R lies.

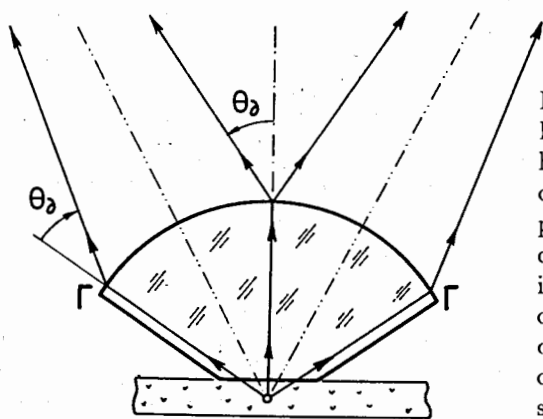
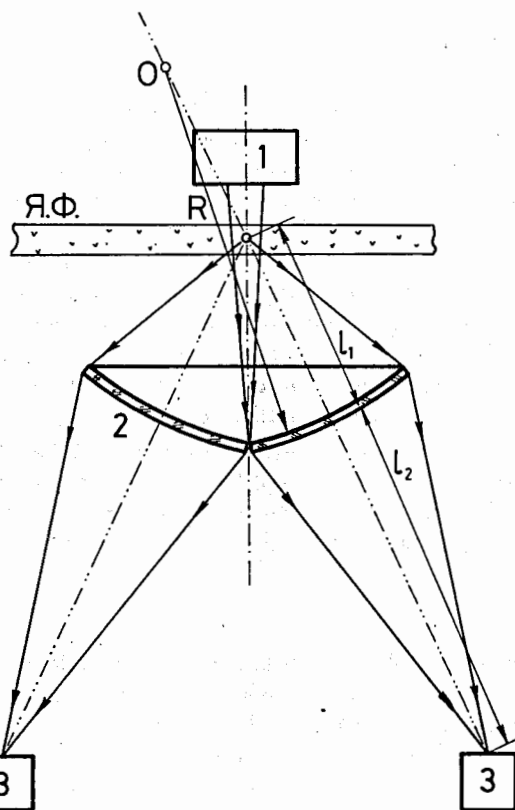


Fig. 2. Basic aplanatic meso-optical hologram Γ with a ring response on the spherical backing: O - the particle track in the median plane of the nuclear emulsion layer, θ_d is the diffraction bending angle of the extreme light rays due to diffraction on the aplanatic meso-optical hologram Γ with a ring response on the spherical backing.

photosensitive layer 3 is casted directly on the spherical surface of the frontal lens 4. In the course of the successive exposition of the photosensitive layer, the frontal lens 4 with photosensitive layer is rotating around its optical axis.

To explain the technological process of the production of this meso-optical hologram with a ring response, we consider a device for production of the equivalent plane hologram with ring response (Fig. 4). The divergent light beam from the point light source 1 is transformed by the positive lens 2 into the convergent light beam. The auxiliary plane hologram 3 produces an additional, divergent, light beam. These two light beams, one divergent and another convergent, are mutually coherent. They generate an interference pattern in the plane of the photosensitive layer 5. The plane shutter 4, provided with very small ($\sim 3^\circ$) open sector aperture, transmits very small part of the whole interference pattern. During the exposition the motor 6 rotates the photosensitive layer 5 and thus provides a successive illumination of all parts of the photosensitive layer 5.

Another more detailed scheme of such a device used for successive exposition of the photosensitive layer is shown in Fig. 5. The light from the light source 1 is collimated by the lens 2. The semitransparent light beam splitter 3 produces two mutually coherent plane waves which are directed onto the lenses 5 and 6 by plane mirrors 4. The lens 5 focuses the light into a point onto the plain microscopic mirror 7, which transforms this light beam into the divergent spherical wave. The lens 6 produces the convergent spherical wave. The Fresnel interference pattern is generated in the region of the mutual overlapping of the divergent and of the convergent spherical waves. This interference pattern is detected on the photosensitive layer 9, which is rotating during the exposition by the motor 10. The sector shutter 8 restricts the instant exposition zone.

The mutual arrangement of the light beams, the sector shutter 8, the photosensitive layer 9 and the motor 10 during the exposition is shown in Fig. 6. Also the structure of the interference picture is presented.

III. MFTM WITH ISOPLANATIC MESO-OPTICAL MIRROR

Now we consider the design of the MFTM provided with isoplanatic meso-optical mirror. The generating line of this axial symmetrical mirror has the multielement structure, each element of which being a short arc of one of the tautochronic ellipses.

By definition, a family of the tautochronic ellipses is specified by two focuses. Two adjacent tautochronic ellipses are separated by the mutual distance and by the wave length of the light λ . To evaluate this distance, we consider the reflection of the light ray, going from the first focus F_1 , at the points A and B, lying on the adjacent tautochronic ellipses (Fig. 7). The reflected light rays AC and BD must be added in phase at the second focus F_2 . Therefore the distance d , which separates two adjacent tautochronic ellipses, must be chosen according to the equation

Fig. 3.
The device for production of the aplanatic meso-optical hologram on the spherical backing: 1 - source of the convergent and divergent light beams, 2 - the shutter with open aperture in the form of a sector, 3 - photosensitive layer mounted on the spherical surface of the frontal lens 4.

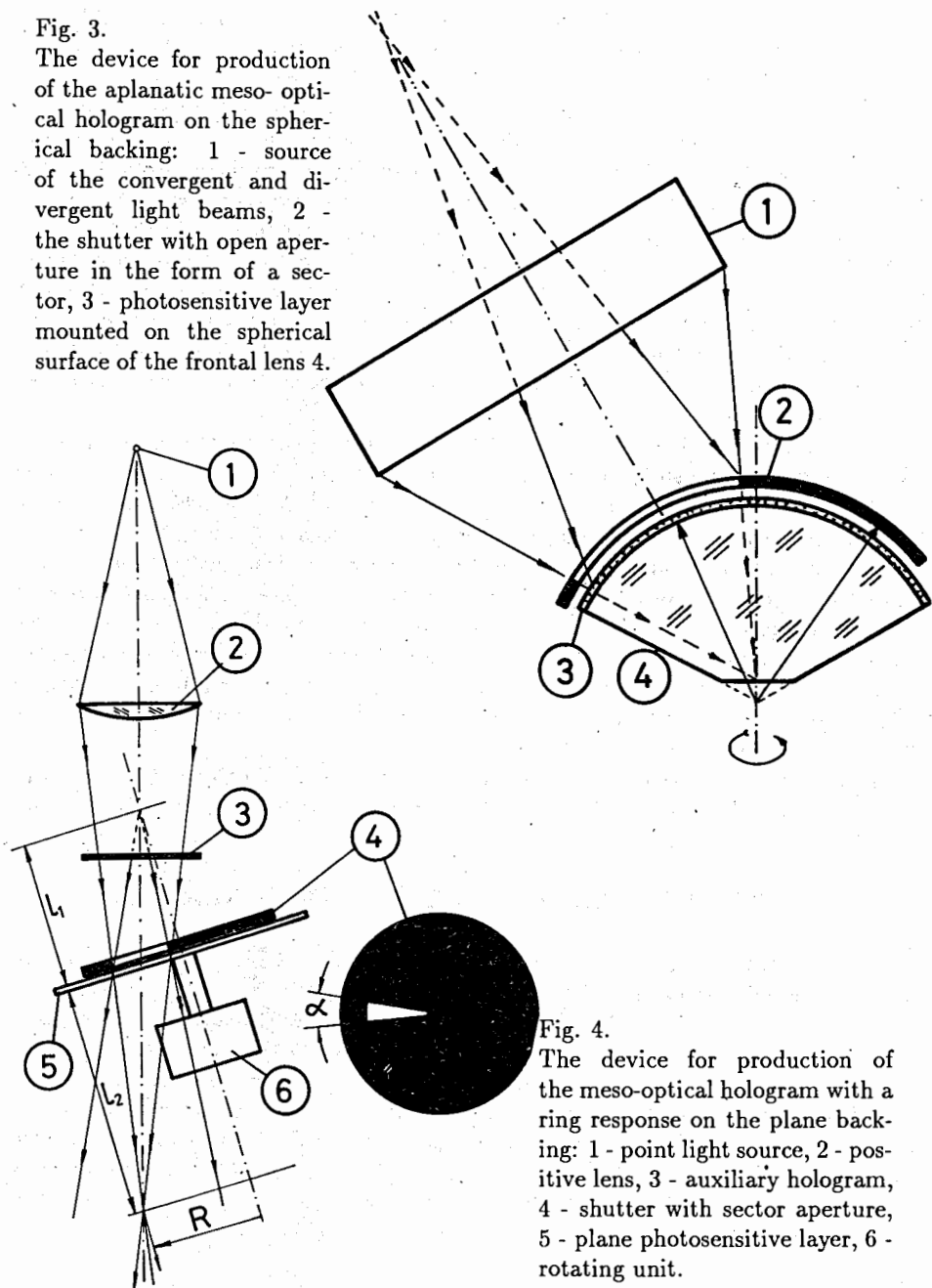


Fig. 4.
The device for production of the meso-optical hologram with a ring response on the plane backing: 1 - point light source, 2 - positive lens, 3 - auxiliary hologram, 4 - shutter with sector aperture, 5 - plane photosensitive layer, 6 - rotating unit.

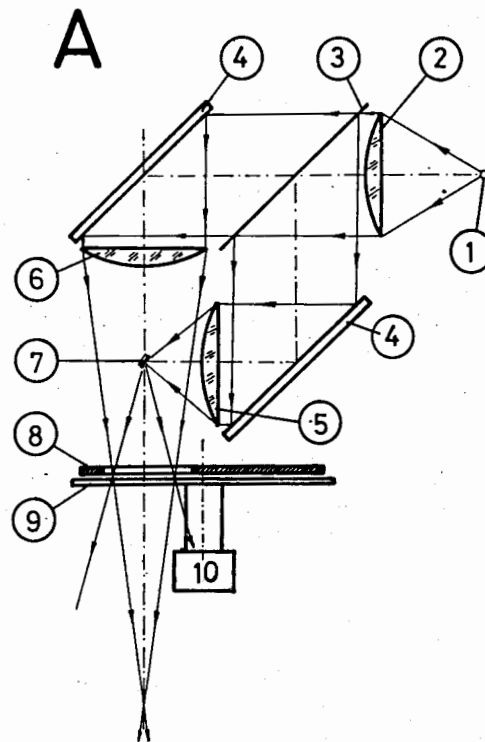


Fig. 5.
More detailed scheme of the device for production of the meso-optical hologram with a ring response on the plane backing: 1 - point light source, 2 - positive lens, 3 - beam splitter, 4 - plane mirror, 5 - positive lens, 6 - positive lens, 7 - microscopic plane mirror, 8 - shutter with sector aperture, 9 - plane photosensitive layer, 10 - rotating unit.

Б

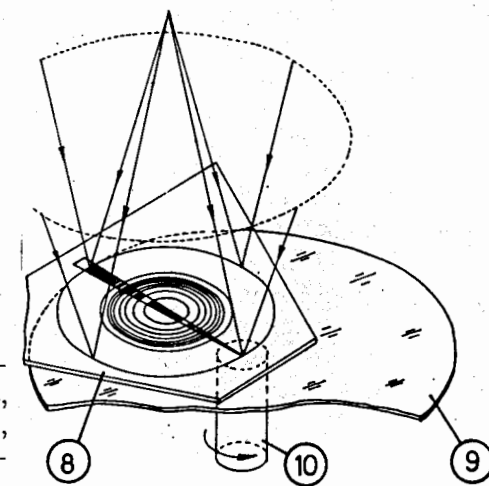


Fig. 6.
The relative arrangement of the convergent and divergent light beams, plane shutter with sector aperture 8, photosensitive layer 9 on the rotating unit 10 (cf. Fig. 5).

$$d = \frac{\lambda}{2} \cdot \frac{1}{\cos \Psi}, \quad (2)$$

where Ψ is the incident angle of the light ray F_1AB . In a small region of two adjacent tautochronic ellipses the angle Ψ and the distance d can be considered as constant factors.

The first focus of our tautochronic ellipses is located at the point F_1 on the optical axis F_1A of the MFTM in the median plane of the nuclear emulsion layer. The second focus of our tautochronic ellipses is located in the point F_2 , where one of two meso-optical images is generated by the meso-optical mirror.

The main feature of the generating line of the isoplanatic meso-optical mirror is that the gravity centers of the reflected elements of this multielement generating line are located on the "carrier ellipse", which is defined by the additional sagitta V :

$$V = \frac{(H^2 + R^2)^2 - H^2(H + 2\Delta)^2}{4H^2(H + 2\Delta)}, \quad (3)$$

where H is the distance along optical axis of the MFTM from the nearest point of the meso-optical mirror to the first focus of the tautochronic ellipses, R is the distance between two foci of the tautochronic ellipses, and Δ is the sagitta of the traditional meso-optical mirror, defined by the equation

$$\Delta = \sqrt{\frac{H^2 + H\sqrt{(H^2 + R^2)}}{2}} - H. \quad (4)$$

The schematic diagram of the new design of the MFTM provided with isoplanatic meso-optical mirror is given in Fig. 8. The convergent light beam from the light source 1 illuminates the nuclear emulsion layer and produces, in the vicinity of the meso-optical mirror with ring response 2, the Fourier transform of the straight line particle track. The meso-optical mirror 2 produces two meso-optical images of the particle track. The right one is detected by the photosensitive matrix detector 4. The signals from this detector are fed to the computer memory block 5. The unit 3 transports the nuclear emulsion layer and generates the position signals. The multielement generating line of the isoplanatic meso-optical mirror is shown in detail inside the circle. Two adjacent elements of this generating line are connected by the nonworking segment. Such jumps give rise to the diffraction order in the place of the meso-optical mirror. To separate the diffraction order from the zero diffraction image we must choose the length Δ_0 of each arc of the tautochronic ellipse according to the inequality

$$\frac{\lambda}{\Delta_0} \cdot l_2 > D, \quad (5)$$

where l_2 is the distance along light ray from the meso-optical mirror to the second focus F_2 of the tautochronic ellipses.

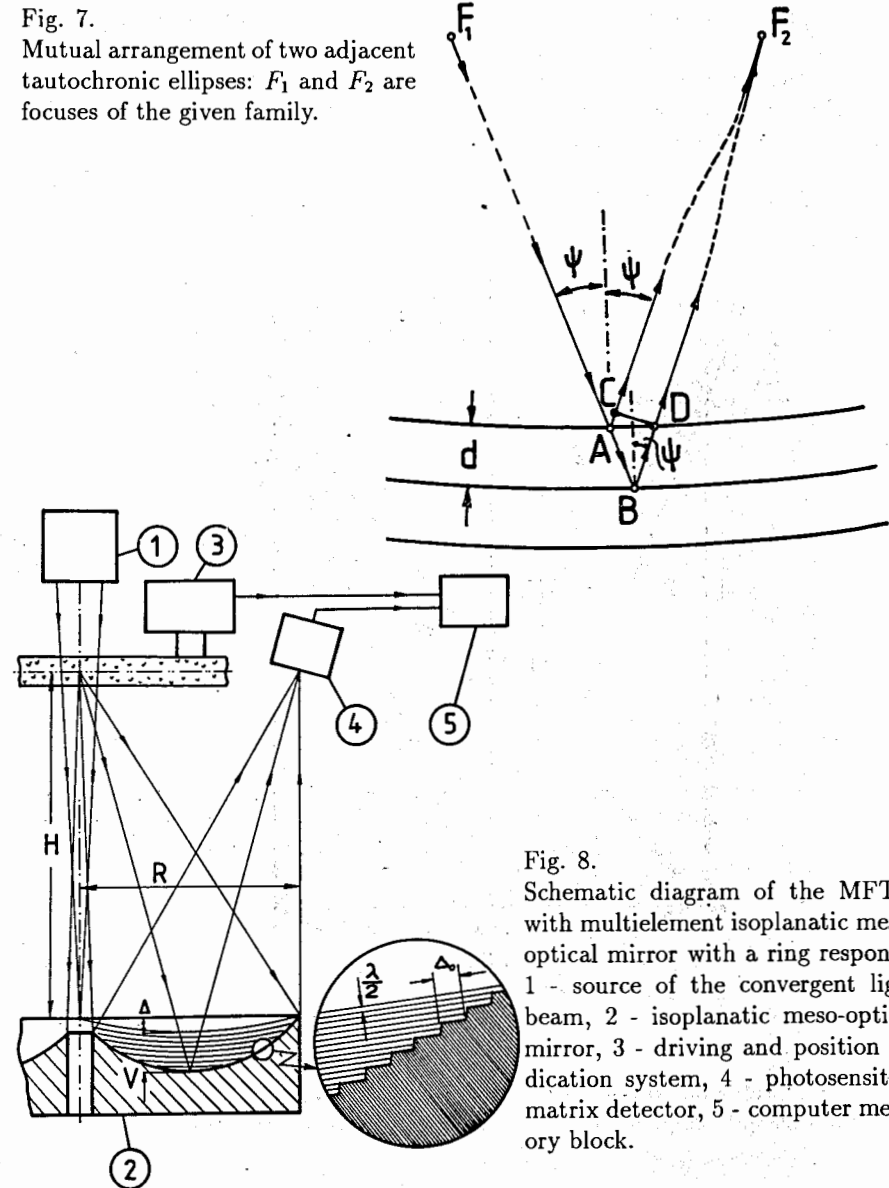


Fig. 8. Schematic diagram of the MFTM with multielement isoplanatic meso-optical mirror with a ring response: 1 - source of the convergent light beam, 2 - isoplanatic meso-optical mirror, 3 - driving and position indication system, 4 - photosensitive matrix detector, 5 - computer memory block.

As

$$\left. \begin{aligned} F_{2q} &= \Delta\gamma \cdot \frac{H^2 + R^2}{R + H\Delta\gamma}, \\ F_{2r} &= F_{2q} \cdot \frac{1}{\operatorname{tg}(\delta - \Delta\gamma)} \end{aligned} \right\} \quad (\text{A.7})$$

where

$$\operatorname{tg}(\delta - \Delta\gamma) = \frac{\frac{H}{R} - \Delta\gamma}{1 + \left(\frac{H}{R}\right)\Delta\gamma} = \frac{HR - \Delta\gamma(H^2 + R^2)}{R^2}. \quad (\text{A.8})$$

From these equations we find:

$$\left. \begin{aligned} x_o &= -H \cdot \Delta\beta, \\ z_o &= -\Delta\beta \cdot H \cdot \operatorname{tg}(\delta - \Delta\gamma) - \Delta\gamma \frac{H^2 + R^2}{R + H\Delta\gamma} \end{aligned} \right\} \quad (\text{A.9})$$

Then we have

$$\mathcal{L} = 2V + \Delta + H = \frac{R}{2} \operatorname{ctg}\Omega_o, \quad (\text{A.10})$$

where

$$\operatorname{ctg}\Omega_o = \frac{z_o}{x_o} = -\frac{[(H^2 + R^2)^2 + H^4 + 2H^3\Delta]}{RH^2(H + 2\Delta)}, \quad (\text{A.11})$$

and

$$\begin{aligned} \mathcal{L} &= \frac{R}{2} \cdot \frac{[(H^2 + R^2)^2 + H^4 + 2H^3\Delta]}{RH^2(H + 2\Delta)} = \\ &= \frac{(H^2 + R^2)^2 + H^3(H + 2\Delta)}{2H^2(H + 2\Delta)}. \end{aligned} \quad (\text{A.12})$$

Finally we calculate the additional sagitta V :

$$\begin{aligned} 2V &= \mathcal{L} - (H + \Delta) = \\ &= \frac{(H^2 + R^2)^2 + H^3(H + 2\Delta)}{2H^2(H + 2\Delta)} - (H + \Delta) = \\ &= \frac{(H^2 + R^2)^2 + H^3(H + 2\Delta) - 2(H^4 + 3H^3\Delta + 2H^2\Delta^2)}{2H^2(H + 2\Delta)}; \end{aligned}$$

or

$$V = \frac{(H^2 + R^2)^2 - H^2(H + 2\Delta)^2}{4H^2(H + 2\Delta)}. \quad (\text{A.13})$$

where the initial sagitta Δ is equal to:

$$\Delta = \sqrt{\frac{H^2 + H\sqrt{H^2 + R^2}}{2}} - H. \quad (\text{A.14})$$

References

1. L.M. Soroko, *Experim. Technik der Physik*, **38**, 401-410, 1990.
2. L.M. Soroko, Preprint JINR, D-13-89-549, Dubna, 1989.
3. Gy.L. Bencze, L.M. Soroko, *Commun. JINR*, P13-86-659, Dubna, 1986.
4. W.T. Welford, *Progress in Optics*, ed. E. Wolf, **13**, 267-292, 1976. North-Holland, Amsterdam.

Received by Publishing Department
on March 30, 1995.